TIJMET, Vol. 004 (2021) 18-31

The International Journal of

Materials and Engineering Technology

ISSN: 2667-4033
TIJMET ID: 210401003 (14 pages)
Type of the Paper: Research Article
Received 17.03.2020 Revised: 31.01.2021 Accepted: 17.02.2021 Published (Online): 06.03.2021
Journal homepage: http://dergipark.gov.tr/tijmet

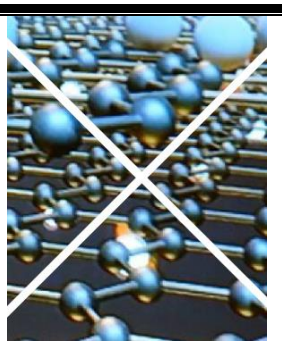

INVESTIGATION OF ACTIVE FAILURE SURFACES OCCURRING BEHIND THE T TYPE CANTILEVER RETAINING WALL

HAKAN ALPER KAMİLOĞLU [1a*], EROL ŞADOĞLU[2b], FATİH YILMAZ[1c]

[1] Bayburt University, Engineering Faculty, Civil Engineering Department, Bayburt, TURKEY.
[2] Karadeniz Technical University, Engineering Faculty, Civil Engineering Department, Trabzon, TURKEY.
[*]hkamiloglu@bayburt.edu.tr

Abstract

Retaining structures are designed considering lateral earth thrust or pressure distribution acting on the wall. Determination of failure surfaces play vital role in active lateral earth pressure calculations acting on retaining structures. As failure surface pattern varies based on heel length, there is particular importance of heel length of T type cantilever retaining walls on determination of earth thrust. Lateral earth calculations are performed for two different cases, namely short heel or long heel, based on the intersection of T type cantilever wall and failure surface. In this study, the effect of heel length on an active failure mechanism was examined with numerical simulation based on finite element method (FEM). The results of the numerical analyses were compared with the results of small-scale model tests and an analytical method. In comparison, the inclination angle of active failure surfaces was taken into account. An earth thrust maximization code suggested in the literature was used to determine failure surface inclination angles analytically. In order to determine failure inclination experimentally, results of small scale tests were used. In the tests, failure surfaces were determined using particle image velocimetry technique (PIV). Numerical analysis was performed using commercially available finite element program Plaxis 2D. The same material properties are used in all numerical models. As a result of the study compatible results with literature was obtained. The effects of heel length, foundation thickness, density parameters on failure surface inclination angles were examined numerically. Due to friction between wall and backfill differences between failure surface inclination angles were determined. Increased heel length caused to decrease of failure surface inclination. However, it was seen that long heel and short heel cases could not be recognized clearly considering the results of numerical analyses.

Keyword: Inverted T cantilever retaining wall, Failure surface, Short heel, Long heel

How to cite this article:
Kamiloğlu, H. A., Şadoğlu, E., Yılmaz, F., Investigation of active failure surfaces occurring behind the T type cantılever retaining wall, The International Journal of Materials and Engineering Technology, 2021, 4(1): 18-31.

ORCID ID:
[a]0000-0003-3313-9239, [b]0000-0003-3757-5126, [c]0000-0002-7962-9834

1. Introduction

Calculations of lateral earth pressure acting on retaining structures are one of the engineering problems that have been encountered since ancient times. The cantilever retaining wall is one of the most commonly used retaining structures in geotechnical engineering and this type of retaining walls have been used since World War II. Different techniques can be used to determine lateral earth thrusts acting on retaining structures, such as the limit equilibrium method [1–4] slip line method, limit analysis method [5-7], stress characteristics method [8-10], zero extension line (ZEL) method [11], numerical methods [12-16], and graphical methods [17,18]. Nonetheless, Coulomb's [19] and Rankine's [20] methods are still used to calculate lateral earth pressure. Common point of the above mentioned methods is considering failure surfaces in earth pressure calculations.

Heel length is a major factor that affecting lateral earth pressure distribution of T type cantilever retaining walls. In various studies, earth pressure calculation methods considering heel length for cantilever retaining walls were suggested [21, 22]. Greco (2008) used terms of 'short heel' and 'long heel' in classification of T type cantilever walls based on heel length. In the active state, active failure surface intersects with stem of the wall in the cases heel length of the wall is not long enough. This type of heel is qualified as short heel. On the other hand, the heel is qualified as long heel when the failure surfaces reach to the backfill surface without intersecting with any obstacle. From the reviewed studies, it is seen that significant differences in failure surface pattern occur based on heel length [21, 22]. In addition, various failure mechanisms occur based on wall geometry [2]. Despite there are wide range of study about earth pressure distribution, the effect of heel length on active failure surface inclination is a gap in the literature. Kamiloglu and Şadoglu (2019) suggested lateral earth thrust and failure surface inclination algorithm considering experimental results. However, small scale tests were considered in lateral earth thrust calculations and the derived earth thrust formulas used developed algorithm. Obtained inclination angle using the suggested algorithm was verified with the same small scale test results. Therefore, it is required to verify the algorithm results with large-scale tests or numerical analyses. In this study it was aimed to examine the effect of heel length, foundation thickness and backfill density on failure surface pattern using numerical approach. The obtained results were compared with experimental and analytical results suggested by Kamiloglu and Şadoğlu (2019).

In this study, it is intended to examine short and long heel phenomena with experimental, analytical and numerical methods. T type cantilever walls can be classified as a short heel or long heel based on the intersection of the cantilever wall and failure surface. Thus, failure surface inclinations should be taken into account in the analyses. Small scale test results performed by Kamiloğlu and Şadoğlu [2] are presented in the experimental part of the study. In the study, active failure surfaces were determined using PIV method. An algorithm suggested by Kamiloğlu and Şadoğlu [2] was used to evaluate active failure surfaces analytically. The algorithm was coded to calculate active earth thrust coefficient and failure surface inclination angles occurring behind inverted T cantilever walls. Analytically derived active earth thrust formulas by Kamiloglu and Şadoğlu [2] were used in the algorithm. Commercially available finite element program Plaxis 2D was used to examine active failure surfaces numerically. Within the scope of the analysis, an inverted T cantilever retaining wall with 3m height was considered. In all analyses, the effect of density, heel length and foundation thickness parameters on failure surface inclinations were examined.

2. Materials and Methods

In this part of the study, examination methods of active failure surfaces are clarified elaborately. The terms used in the study are presented in Fig. 1. In the study, wall length, foundation thickness and heel length were represented with H, H_3, and b respectively. Active failure surface inclination angles were represented with ψ and θ as it is shown in the figure.

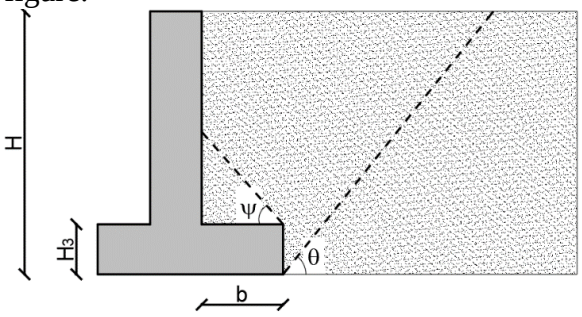

Figure 1. Terms used in the study.

In the study, active failure surfaces occurring behind a cantilever retaining wall was determined with finite element analyses and compared with experimental and analytical results performed by Kamiloglu and Sadoglu [2]. Experimental and analytical analyses [2] were clarified in first part of the study. Finite element models were explained in detail in the second part and results of the analyses were compared with Kamiloglu and Şadoğlu [2].

2. 1. Experimental Examination of Active Failure Surfaces

In this part, small-scale tests performed by Kamiloglu and Şadoğlu [2] are clarified. Backfill material used in the tests was classified as poorly graded sand considering USCS. Crushed sand manufactured by Limak Co. was used as a backfill material. Some granulometric properties of the backfill sieved from 2 m diameter sieve are given in Table 1.

In context of the small-scale test the effect of heel length, foundation thickness and backfill density (or friction angle) on inclination angles of active failure surfaces were examined. A model wall made of hard wood with 0.30 m height was used in the small-scale tests. The walls with 0.03m, 0.06m, 0.09m, 0.12m and 0.15m length were used to examine relation between heel length and failure surface inclinations. Three different foundation thicknesses (0.03m, 0.06m and 0.09 m) were used to examine the effect of foundation thickness on failure surface inclinations. The small-scale tests were performed for three different backfill densities (ρ_1=1.45 Mg/m^3, ρ_2=1.58 Mg/m^3, ρ_3=1.65 Mg/m^3) to examine density-failure surface inclination relations. Heel length and foundation thickness of the model wall used in the tests were 0.06 m and 0.03 m respectively.

To determine active failure surfaces the model wall was subjected to horizontal translation during the tests and active translation recorded with a digital camera. Particle image velocity (PIV) analysis was performed using captured images. The image sequences obtained from the small-scale tests were analyzed with PIVlab, and, the displacement vector fields and the simple strain-rate fields were determined. The inclination angle of the failure surfaces was determined using the results of the PIV analyses. Some geotechnical parameters of the back fill such as density, internal friction angle, modulus of elasticity and friction angles are summarized in Table 2. The parameters were used to determine active inclination angles using numerical, analytical and experimental approaches.

Table 1. Some granulometric properties of backfill soil [2]

Property	Value
D_{10}	0.55 mm
D_{30}	0.75 mm
D_{50}	0.95 mm
D_{60}	1.20 mm
Coefficient of uniformity (Cu)	2.18
Coefficient of gradation (Cc)	0.85
Average specific gravity (Gs)	2.50

Table 2. Some basic properties of backfill soil

Property	Value
Maximum density (ρ_{max})	1.67 Mg/m^3
Minimum density (ρ_{min})	1.41 Mg/m^3
Internal friction angle [ρ_1= 1.45 Mg/m^3]	ϕ=36°
Internal friction angle [ρ_2= 1.58 Mg/m^3]	ϕ=38°
Internal friction angle [ρ_3= 1.65 Mg/m^3]	ϕ=40°
Modulus of elasticity [ρ_1 = 1.45 Mg/m^3]	25.6 MPa
Modulus of elasticity [ρ_2= 1.58 Mg/m^3]	36.6 MPa
Modulus of elasticity [ρ_3= 1.65 Mg/m^3]	47.5 MPa
Friction angle [wall backfill; ρ_1 = 1.45 Mg/m^3]	δ=32°
Friction angle [wall backfill; ρ_2 = 1.58 Mg/m^3]	δ=35°
Friction angle [wall backfill; ρ_3 = 1.65 Mg/m^3]	δ=36°

2.2. Analytical Examination of Active Failure Surfaces

Earth thrust determination method suggested by Kamiloğlu and Şadoğlu [2] for the T type cantilever retaining walls is taken into account in the analytical part of the study. Thus, an algorithm suggested by Kamiloglu and Şadoğlu [2] (Fig.2) is used to predict the inclination angles of the active failure surfaces. In order to compare analytical results with the results of the other methods, the same heel length and foundation thickness coefficient, internal friction angle, density parameters with the experimental study is used.

2.3. Numerical Examination of Active Failure Surfaces

Plaxis 2D 8.6 finite element software was used to examine failure surface behind a cantilever retaining wall with various heel length, foundation thickness and different backfill densities numerically. In the numerical model, retaining walls with 3 m height were considered. In order to create compatible wall geometries with analytical and experimental studies the heel lengths are determined as 0.3m, 0.6m, 0.9m, 1.2m, 1.5m and foundation thicknesses are determined as 0.3m, 0.6m and 0.9m. Beside, same backfill properties with experimental study is considered in the finite element (FE) analyses. Optimum lateral and vertical dimensions for the model were determined to establish the model properly. Therefore, horizontal and vertical dimensions of the model were determined as 8m and 6m to provide adequate dimension failure surfaces freely develop. Displacements of the vertical boundaries (vertical direction) and bottom boundaries (vertical and horizontal directions) of the model was constrained. Active state was created by translating the model wall horizontally away from the backfill. The horizontal movement was determined as 0.1% of the wall height. In the analyses Mohr-Coulomb material model and fifteen noded triangular elements with three Gauss points were used. Friction effect occurring between the wall and backfill was simulated with interface elements. Backfill properties shown in Table 1 are taken into account in the FE analyses. Additionally, other parameters used in the FE analyses are presented in Table 3. The effect of friction was simulated with δ/φ value. By taking into consideration the suggestions of Kamiloğlu et.al. [23] average element size of the model is determined as 70.16 x10^{-3} m (Fig.2b). In modelling process, it was not enable to neglect cohesion parameters. Therefore, cohesion parameter was determined as 0.1 kN/m^2 to simulate granular material.

The mesh size of the element is refined locally around the backfill and the wall, particularly near the contact surfaces between the wall and backfill. As a result of the FE analyses strain fields and failure surface inclinations are determined.

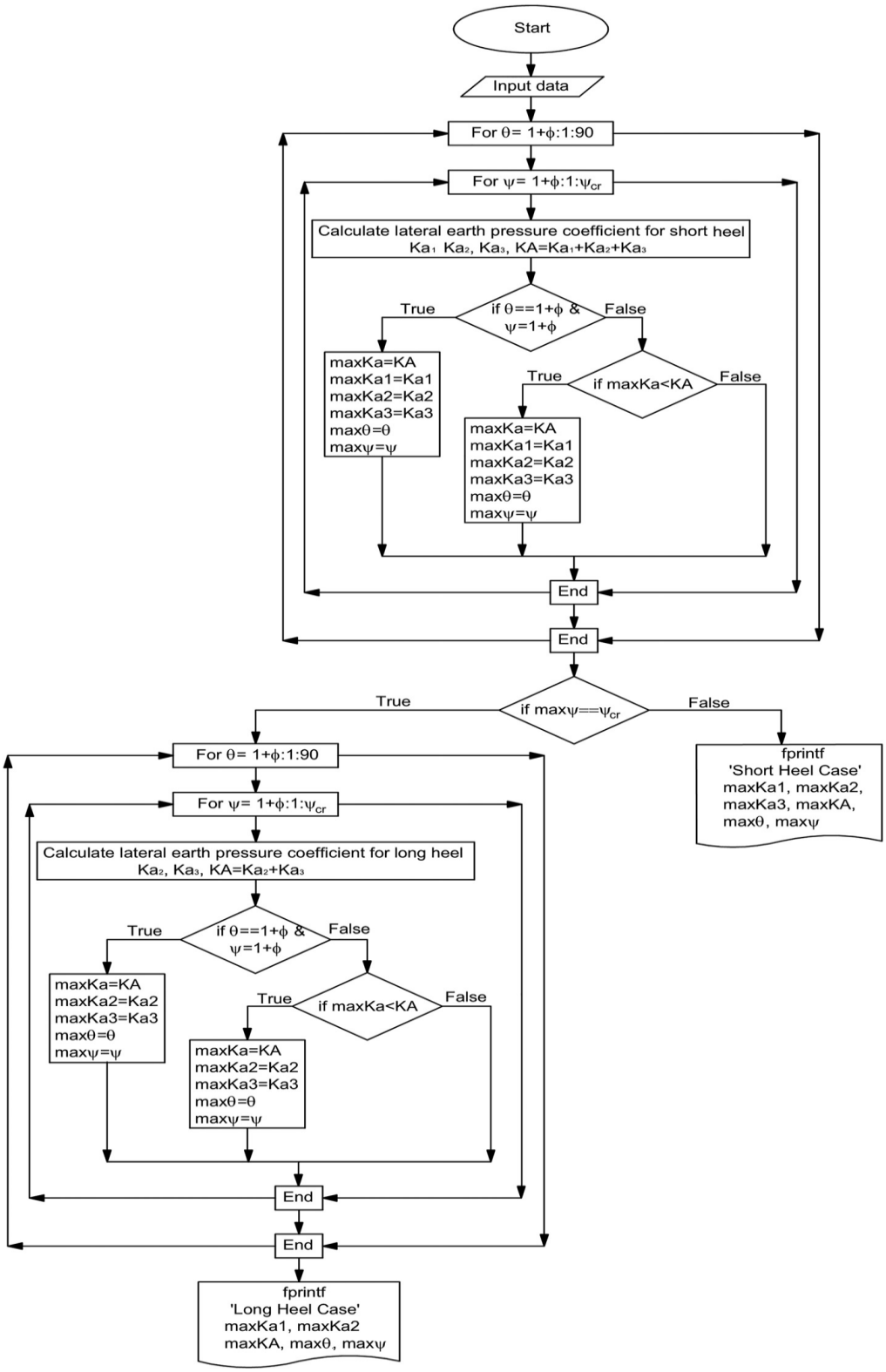

Figure 2. Flowchart of thrust-maximization algorithm [2]

Table 3. Parameters considered in the FE analyses

ϕ	Property	Value	ϕ	Property	Value	ϕ	Property	Value
36°	E	25.6 MPa	38°	E	36.6 MPa	40°	E	47.5 MPa
	υ	0.3		υ	0.3		υ	0.3
	γ_{unsat}	14.5 kN/m^3		γ_{unsat}	15.8 kN/m^3		γ_{unsat}	16.5kN/m^3
	γ_{sat}	18.7 kN/m^3		γ_{sat}	19.5 kN/m^3		γ_{sat}	19.96kN/m^3
	δ	32°		δ	35°		δ	36°
	R_{inter}	0.888		R_{inter}	0.92		R_{inter}	0.9
	c	0.1 kN/m^2		c	0.1 kN/m^2		c	0.1 kN/m^2

E: Modulus of elasticity, ν: Poisson's ratio, δ: friction angle, c: cohesion, R_{inter}: stress reduction factor, ϕ: internal friction angle, γ_{sat}: saturated unit weight, γ_{unsat}: moist unit weight

Figure 3 shows the results of the FE analyses performed to obtain failure surfaces occurred behind the wall for various heel lengths. In the FE analyses, heel lengths of the walls were determined as 0.3m ,0.6m ,0.9m ,1.2m,1.5m and foundation thickness was 0.3 m. Internal friction angles and density parameters of the backfill soil modeled in the analyses were, 36° and 1.45 Mg/m^3 respectively.

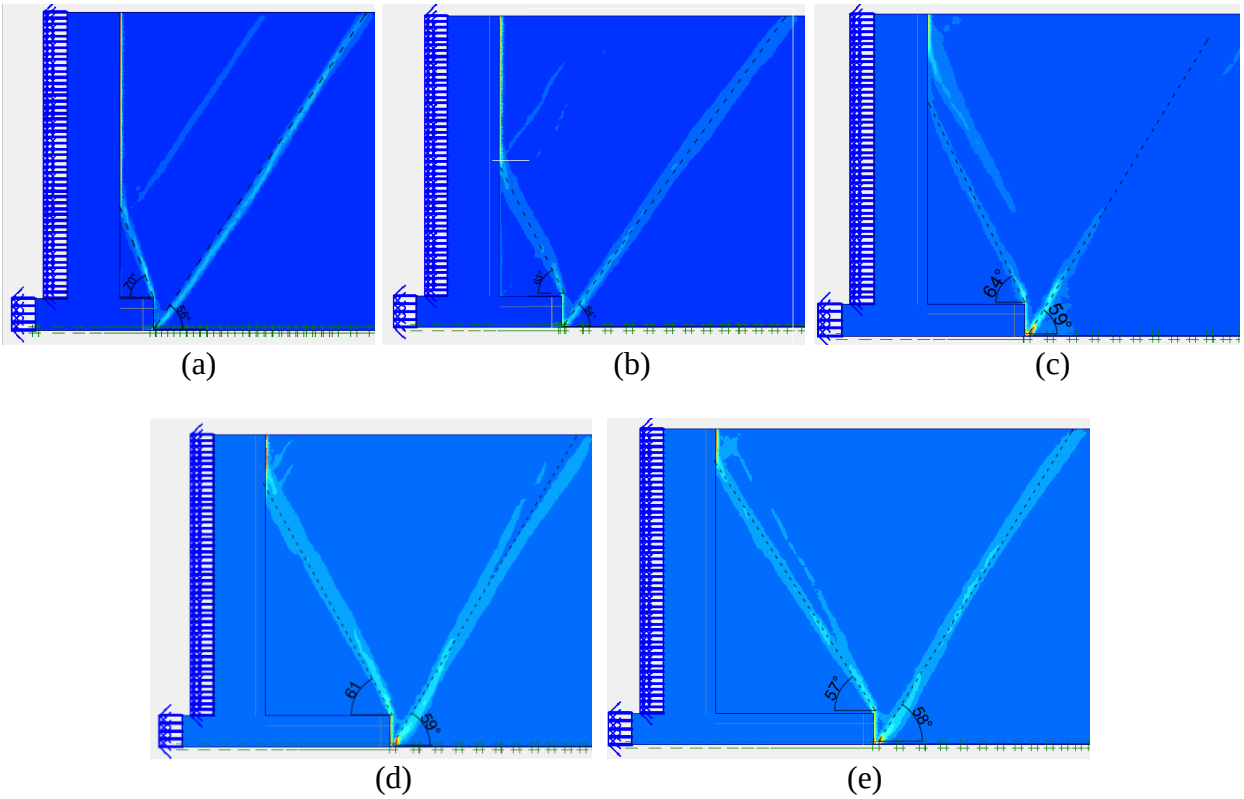

Figure 3. Inclination angles of failure surfaces for various heel lengths, (a) b=0.3m, H_3=0.3 m; (b) b=0.6m, H_3=0.3 m; (c) b=0.9m, H_3=0.3 m; (d) b=1.2m, H_3=0.3 m; (e) b=1.5m, H_3=0.3 m.

Results of PIV analyses performed by Kamiloglu and Sadoglu [2] are presented in Figure 4. In the analyses, b/H and H_3/H ratios were represented with β and α respectively. The figures show change of active failure surface patterns with increasing heel lengths.

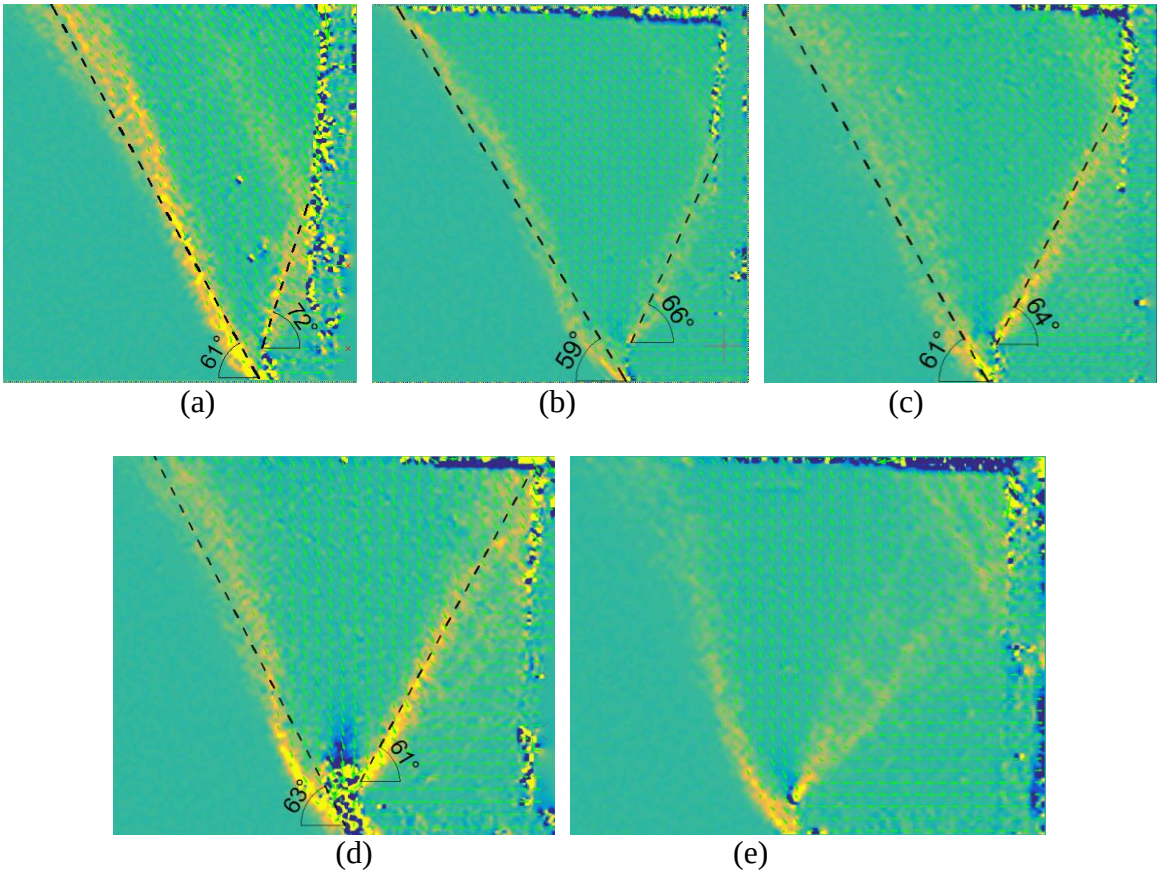

Figure 4. Experimentally determined failure surface inclinations for various heel lengths [2] α=0.1, ϕ=36° a) β=0.1, b) β=0.2, c) β=0.3, d) β=0.4, e) β=0.5

In Figure 5, the effect of heel length on active failure surface pattern is shown. The analyses were performed for the 0.6 m thick foundation. Failure surface inclination angles were presented for the wall with various heel lengths.

The results of experimental analyses are seen in Figure 6. In the experimental analyses internal friction angle of the backfill and H_3/H ratio were determined as 36 ° and 0.2 respectively. From the figures change of active failure surface pattern with various heel lengths are seen. In the analyses β=b/H ratio was used to represent heel length. The heel lengths coefficients of the walls were determined as β=0.1, 0.2, 0.3, 0.4 and 0.5.

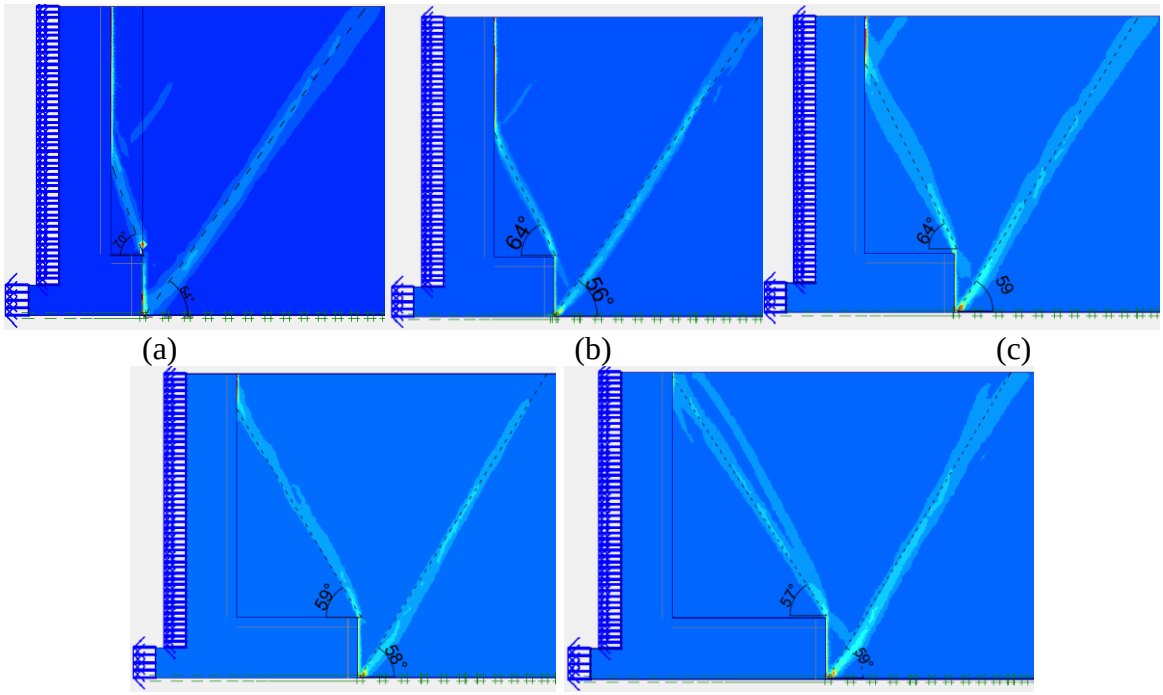

Figure 5. Inclination angles of failure surfaces for various heel lengths, (a) b=0.3m, H_3=0.6m; (b) b=0.6m, H_3=0.6 m; (c) b=0.9m, H_3=0.6m; (d) b=1.2m, H_3=0.6 m; (e) b=1.5m, H_3=0.6 m.

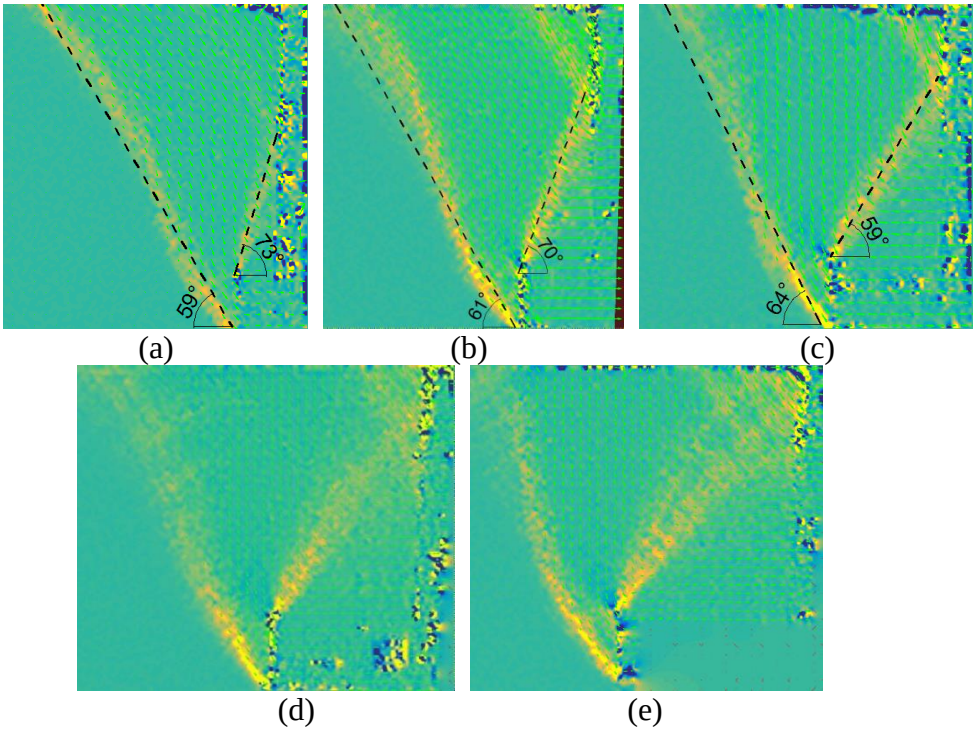

Figure 6. Experimentally determined failure surface inclinations for various heel lengths [2] α=0.2, ϕ=36° a) β=0.1, b) β=0.2, c) β=0.3, d) β=0.4, e) β=0.5

In Figure 7, results of the FE analyses for the wall with 0.9m foundation thickness and different heel lengths (0.3m, 0.6m, 0.9m, 1.2m and 1.5m) are shown.

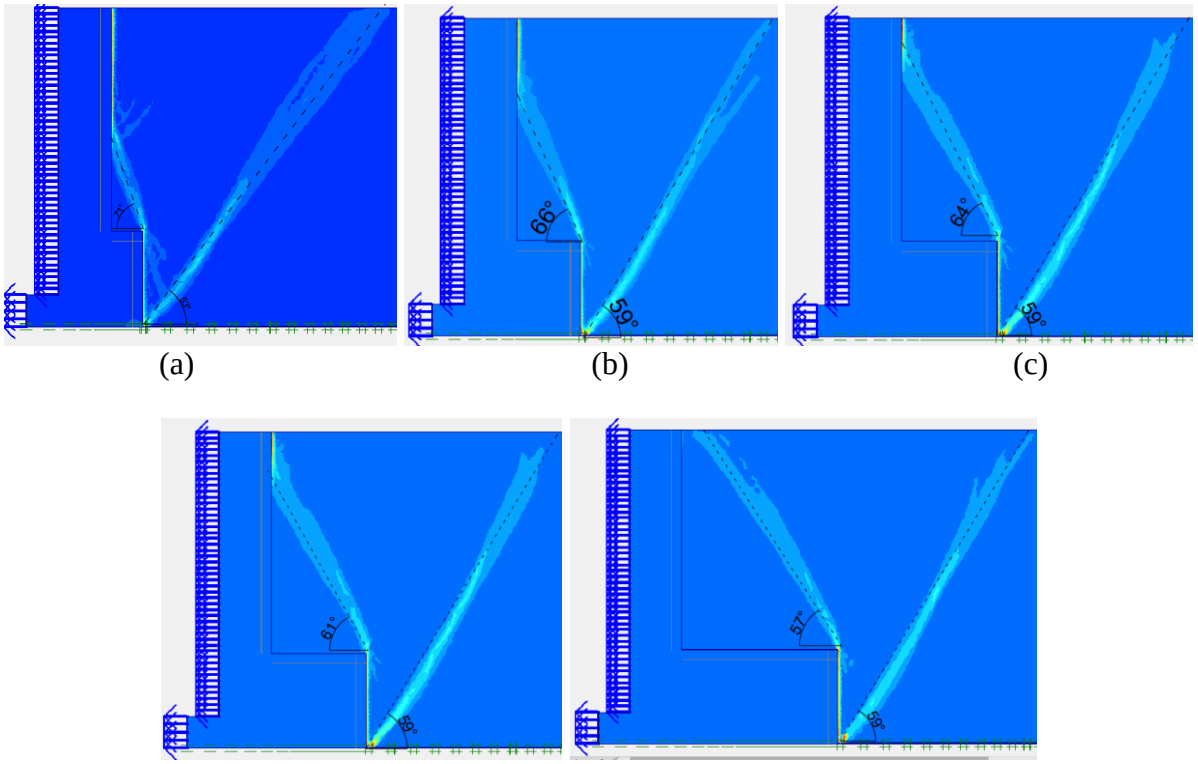

(a) (b) (c)

(d) (e)

Figure 7. Inclination angles of failure surfaces for various heel lengths, (a) b=0.3m, H_3=0.9 m; (b) b=0.6m, H_3=0.9 m; (c) b=0.9m, H_3=0.9 m; (d) b=1.2m, H_3=0.9 m; (e) b=1.5m, H_3=0.9 m.

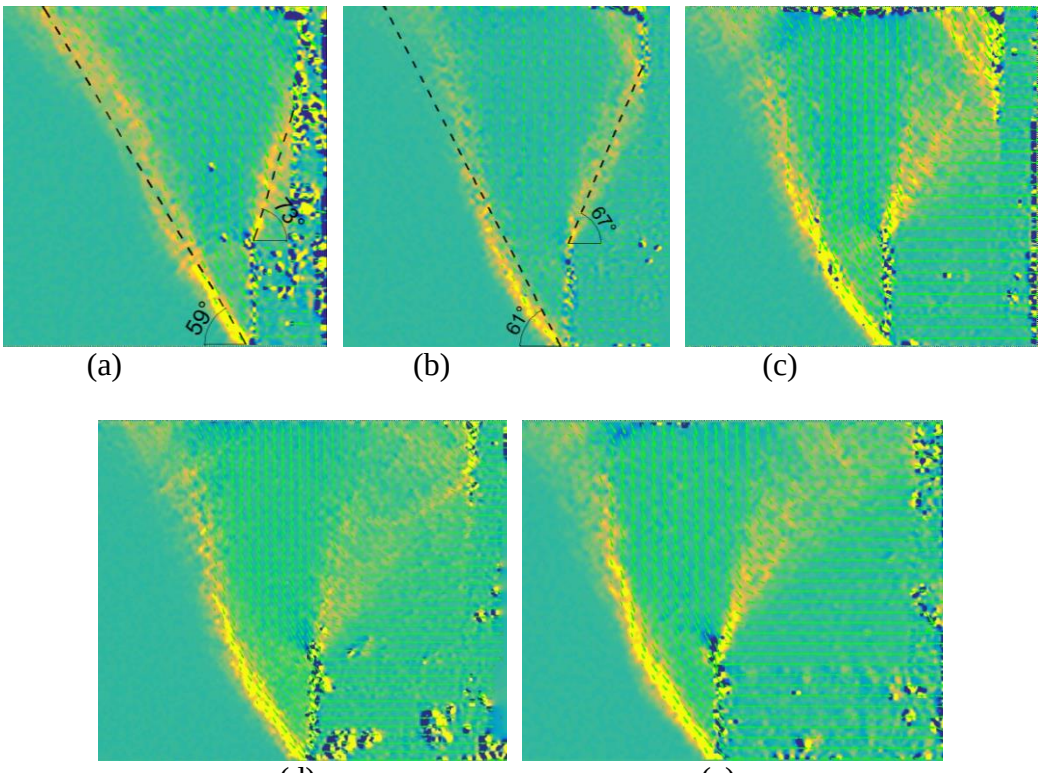

(a) (b) (c)

(d) (e)

Figure 8. Experimentally determined failure surface inclinations for various heel lengths [2] α=0.2, ϕ=36° a) β=0.1, b) β=0.2, c) β=0.3, d) β=0.4, e) β=0.5

Figure 8 represents the results of the experimental analyses performed for various heel length coefficients. In the analyses internal friction angle of the backfill and H_3/H ratio were determined as 36° and 0.3 respectively.

In order to examine effect of density on failure surface inclinations internal friction angles were used. Internal friction angles of the sand compacted with various densities (ρ_1= 1.45 Mg/m^3, ρ_2= 1.53, and ρ_3= 1.65 Mg/m^3) were determined as ϕ = 36°, 38°, 40°. Heel length and foundation thickness of the cantilever retaining wall are 0.06 m and 0.03m respectively. The effect of backfill density on active failure surface geometry is presented in Figure 9.

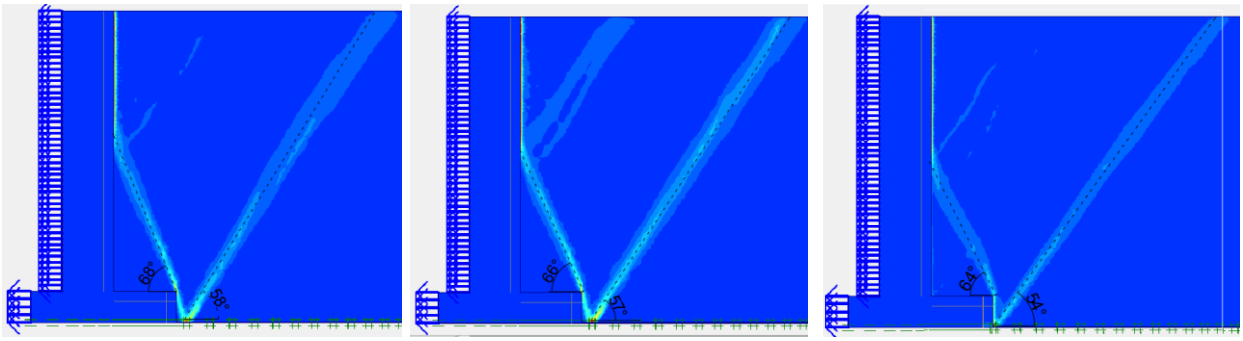

(a) (b) (c)

Figure 9. Inclination angles of failure surfaces for various densities (α =0.3 m, β =0.6 m): (a) ρ=1.45 kN/m^3 (ϕ=36°); (b) ρ=1.53 kN/m^3 (ϕ=38°); (c) ρ=1.65 kN/m^3 (ϕ=40°).

3. Results and Discussion

Results of the analytical, numerical and experimental studies are shown in Table 4, Table 5 and Table 6. After horizontal translation of the wall, two active failure surfaces occur behind the wall. The inclination angle of the failure surface occurring close to the wall is termed as angle ψ and the inclination angle of the failure surface occurring at the far point of the wall is termed as angle θ. The effect of heel length coefficient and foundation thickness coefficient on angle ψ and angle θ is shown in Table 4 and Table 5 respectively. Also, the results of the FE analyses are compared with the results of the analytical and experimental [2] studies and Rankine's method [21].

From Table 4 it is seen that the results of the numerical study are compatible with the results of experimental and analytical study [2]. Angle ψ values determined with analytical, experimental and numerical approaches decreased with increasing heel length up to a constant heel length value. Slight differences between the method occurred in estimation of failure inclinations for β>0.4. Angle ψ obtained with experimental, analytical and numerical methods are effected from the heel length and foundation thickness coefficients. On the other hand, the inclination angle of the failure surface found by using Rankine's method is not affected by the heel length or foundation thickness parameters.

Table 4. ψ angles determined with various approaches

Foundation thickness coefficient	Method	Heel Length Coefficient				
		β=0.1	β=0.2	β=0.3	β=0.4	β=0.5
α=0.1	Experimental Study [2]	72°	66°	64°	61°	DFS
	Analytical Study [2]	74°	70°	67°	64°	63°(LH)
	Numerical Study	70°	63°	64°	61°	57°
	Rankine (45+ϕ/2)	63°	63°	63°	63°	63°
α=0.2	Experimental Study [2]	73°	70°	59°	DFS	DFS
	Analytical Study [2]	73°	69°	66°	63°(LH)	63°(LH)
	Numerical Study	70°	64°	64°	59°	57°
	Rankine (45+ϕ/2)	63°	63°	63°	63°	63°
α=0.3	Experimental Study [2]	73°	67°	DFS	DFS	DFS
	Analytical Study [2]	73°	68°	65°	63°(LH)	63°(LH)
	Numerical Study	71°	66°	64°	61°	57°
	Rankine (45+ϕ/2)	63°	63°	63°	63°	63°

DFS=dispersed failure surface, LH=long heel.

The angle θ determined with various methods is presented in Table 5. It is seen from the table that wall dimensions have negligible effects on the angle θ. In addition, long heel or short heel cases can be defined with analytical and experimental studies. However, this cases cannot be defined using numerical methods and Rankine's methods.

Table 5. θ angles determined with various approaches

Foundation thickness coefficient	Method	Heel Length Coefficient				
		β=0.1	β=0.2	β=0.3	β=0.4	β=0.5
α=0.1	Experimental Study [2]	61°	59°	61°	63°	DFS
	Analytical Study [2]	60°	61°	62°	62°	63°(LH)
	Numerical Study	56°	54°	59°	59°	58°
	Rankine (45+ϕ/2)	63°	63°	63°	63°	63°
α=0.2	Experimental Study [2]	59°	61°	64°	DFS	DFS
	Analytical Study [2]	60°	61°	61°	61°(LH)	61°(LH)
	Numerical Study	54°	56°	59°	58°	59°
	Rankine (45+ϕ/2)	63°	63°	63°	63°	63°
α=0.3	Experimental Study [2]	59°	61°	DFS	DFS	DFS
	Analytical Study [2]	53°	59°	58°	59°	59°
	Numerical Study	60°	60°	60°	60°(LH)	60°(LH)
	Rankine (45+ϕ/2)	63°	63°	63°	63°	63°

DFS=dispersed failure surface, LH=long heel.

Inclination angles of the active failure surfaces (angles ψ and θ) determined using different methods are seen in Table 6. The failure surface inclination angles are examined for various backfill densities. As it is seen from the table, backfill density (or internal friction angle) has considerable effects on failure surface inclination angles (angle ψ and θ).

Table 6. Effect of density on angle ψ and angle θ

Density (Mg/m^3)	ρ_1= 1.45		ρ_2=1.58		ρ_3=1.65	
Method	ψ	θ	ψ	θ	ψ	θ
Experimental Study [2]	66°	59°	66°	71°	67°	77°
Analytical Study [2]	70°	61°	70°	62°	71°	63°
Numerical Study	64°	55°	66°	57°	68°	58°
Rankine (45+ϕ/2)	63°	63°	64°	64°	65°	65°

4. Conclusions

In this study, active failure surfaces occurring behind inverted T cantilever retaining walls are examined considering various methods. In the examination of the failure surfaces, inclination angles are taken into account. The FE analyses were performed for the wall with different heel lengths, foundation thicknesses and backfill densities. The numerical results are compared with the results of the small-scale tests [2], an algorithm coded to determine active failure surface inclination angles [2] and Rankine's method [20]. As a result of the study the following conclusions may be drawn:

- As a result of the numerical study it is seen that heel length and foundation thickness have considerable effects on the inclination angle of the active failure surface occurring at the close point of the wall (angle ψ). On the other hand, the inclination angle of the active failure surface occurring at the far point of the wall (angle θ) is not affected by the heel length or foundation thickness.
- Long heel and short heel cases could not be recognized clearly considering the results of numerical analyses.
- The effect of heel length and foundation thickness parameters on the inclination angles of the active failure surfaces cannot be determined with Rankine's method.
- Backfill density and internal friction of the backfill have considerable effects on active failure surfaces.
- As a result of the FE analyses, it was seen that the backfill density has a slight effect on failure surfaces inclination angles.

Acknowledgments

The authors would like to express their deepest appreciation to organizing committee of TICMET19 in the selection of their study which was presented in the conference organized on 10-12 October, 2019 in Gaziantep University

References

1. Rahardjo, H., and Fredlund, D.G. General limit equilibrium method for lateral earth force, Canadian Geotechnical Journal. **2011**, 21(1):166-175, DOI: 10.1139/t84-013.
2. Kamiloğlu, H. A. and Şadoğlu, E. Experimental and theoretical investigation of short and long heel cases of cantilever retaining walls in active state, Int. J. Geomech., **2019**, 19(5): 04019023, DOI: 10.1061/(ASCE)GM.1943-5622.0001389.
3. Ouyang, C., Xu, Q., He, S., Luo, Y. and Wu,Y. A generalized limit equilibrium method for the solution of active earth pressure on a retaining wall, Journal of Mountain Science, **2019**, 10(6):1018-1027, DOI: 10.1007/s11629-013-2576-x.
4. Cao, W., Liu, T., Xu, Z. Estimation of active earth pressure on inclined retaining wall based on simplified principal stress trajectory method, Int. J. Geomech., **2019**, 19(7): 06019011, DOI: 10.1061/(ASCE)GM.1943-5622.0001447.

5. Liu, X.R., Xi, O.M., and Yang, X. Upper bound limit analysis of passive earth pressure of cohesive backfill on retaining wall, Applied Mechanics and Materials, **2013**, 353-356:895-900, DOI:10.4028/www.scientific.net/AMM.353-356.895.
6. Farzaneh, O., Askari, F., and Fatemi, J. Active earth pressure induced by strip loads on a backfill, Int. J. Civ. Eng., **2013**, 12(4):281-291.
7. Chen, W.F., and Rosenfarb, J.L. Limit analysis solutions of earth pressure problems. Soils Found., **1973**, 13(4): 45-60.
8. Keshavarz, A., and Ebrahimi, M. Axisymmetric active lateral earth pressure for c-Φ soils using the stress characteristics method. Scientia Iranica A. **2017**, 24(5): 2332-2345, DOI:10.24200/sci.2017.4155
9. Keshavarz, A., and Ebrahimi, M. The effects of the soil-wall adhesion and friction angle on the active lateral earth pressure of circular retaining walls, Int. J. Civ. Eng. **2016**, 14: 97-105, https://doi.org/10.1007/s40999-016-0016-3
10. Kumar, J., and Chitikela, S. Seismic passive earth pressure coefficients using the method of characteristics, Canadian Geotechnical Journal, **2002**, 39(2): 463-471, https://doi.org/10.1139/t01-103
11. Anvar, S.A., and Ghahramani, A. Dynamic active earth pressure against retaining walls, Proceedings: Third International Conference on Recent Advances in Geotechnical Earthquake Engineering and Soil Dynamics, **2013**, St Louis, Missouri, USA.
12. Hu, W., Liu, K., Zhu, X., Tong, X., and Zhou, X. Active earth pressure against rigid retaining walls for finite soils in sloping condition considering shear stress and soil arching effect, Hindawi Advances in Civil Engineering, **2020**, https://doi.org/10.1155/2020/6791301.
13. Hamidi, P., Akhlaghi, T., and Bonab, M.H. Finite element limit analysis of active earth pressure in nonhomogeneous soils, Acta Universitatis Agriculturae et Silviculturae Mendelianae Brunensis, **2016**, 64(4):1131-1138, DOI: 10.11118/actaun201664041131.
14. Tang, L., Cong, S., Xing, W., Ling, X., Geng, L., and Gan, F. Finite element analysis of lateral earth pressure on sheet pile walls, Engineering Geology, **2018**, 244:146-158, https://doi.org/10.1016/j.enggeo.2018.07.030.
15. Hsin, K., and Liu, C.N. Finite element analysis of earth pressures for narrow retaining walls, Journal of GeoEngineering, **2007**, 2(2):43-52, DOI: 10.6310/jog.2007.2(2).1
16. Fan, C.C., and Fang, Y.S. Numerical solution of active earth pressures on rigid retaining walls built near rock faces, Computers and Geotechnics, **2010**, 37:1023-1029, DOI:10.1016/j.compgeo.2010.08.004
17. Lu, H., and Yuan, B. Calculation of passive earth pressure of cohesive soil based on Culmann's method, Water Science and Engineering, **2011**, 35(1): DOI:10.3882/j.issn.1674-2370.2011.01.010
18. Thakur, A.K., and Chattopadhyay, B.C. Active earth pressure on cohesion-less soil: theoretical and graphical considerations, Environmental Science, **2017**, DOI:10.14445/22315381/IJETT-V49P260
19. C. A. Coulomb, Essai Sur Une Application Des Règles de Maximis & Minimis à Quelques Problèmes de Statique, Relatifs à L'architecture, des Sci. Mem. MATh. Phys. Par Divers Savants, **1776**, 7: 343–382.
20. Rankine, W.J.M., On The Stability of Loose Earth, Phil. Trans. Royal Soc.,**1857**, 147.

21. Greco, V.R., Analytical active earth thrust on cantilever walls with short heel, Canadian Geotechnical Journal, **2008**, 45(12): 1649-1658, DOI: 10.1139/T08-078
22. Goh, A.T.C. Behavior of cantilever retaining walls, J. Geotech. Eng. **1993**, 119(11): 1751-1770.
23. Kamiloğlu, H.A., Şadoğlu, E., and Yılmaz, F. Numerical analysis of active earth pressures on inverted T Type and semi-gravity walls. 3rd International Conference on Advanced Engineering Technologies, **2019**, Bayburt, Turkey